International Journal of Mass Spectrometry 290 (2010) 22–31

Contents lists available at ScienceDirect

International Journal of Mass Spectrometry

journal homepage: www.elsevier.com/locate/ijms

Coordination chemistry of nickel(II) nitrate with superbasic guanidines as studied by electrospray mass spectrometry

Zoran Glasovac[a,*], Vjekoslav Štrukil[a], Mirjana Eckert-Maksić[a], Detlef Schröder[b,*], Maria Schlangen[c], Helmut Schwarz[c]

[a] Division of Organic Chemistry and Biochemistry, Ruđer Bošković Institute, POB 180, HR-10002 Zagreb, Croatia
[b] Institute of Organic Chemistry and Biochemistry, Flemingovo nám. 2, 16610 Prague6, Czech Republic
[c] Institut für Chemie, Technische Universität Berlin, Strasse des 17. Juni 135, 10623 Berlin, Germany

ARTICLE INFO

Article history:
Received 2 September 2009
Received in revised form
13 November 2009
Accepted 15 November 2009
Available online 20 November 2009

Keywords:
Electrospray ionization
Guanidine
Ion association
Nickel(II) nitrate
Solvation

ABSTRACT

The coordination chemistry of nickel(II) nitrate with four guanidines bearing heteroatom-containing alkyl sidechains is investigated by means of electrospray ionization mass spectrometry of dilute methanolic solutions. In contrast to other nitrogen bases, the ESI spectra of the solutions containing superbasic guanidines are dominated by signals due to the protonated nitrogen bases, BH^+. Under soft ionization conditions, also several nickel-containing ions are observed which are best described as complexes between the guanidinum ions BH^+ with neutral nickel(II) nitrate coordinated via the nitrato ligands in terms of ion pairs. For guanidine derivatives with at least two *N*,*N*-dimethylaminopropyl groups in the sidechains, also the formation of genuine amino-nickel complexes is inferred. The pronounced difference between the ions formed upon ESI of aqueous nickel(II) nitrate in the presence of guanidines compared to other, weaker nitrogen bases is ascribed to the high basicity of the guanidines, which renders their protonation much more favored than their possible operation as ligands for the metal center.

1. Introduction

The gas-phase coordination chemistry of nickel cations has been studied in great detail [1] and has been reviewed recently [2]. Much like other transition metals, nickel has a high affinity to nitrogen ligands and the coordination chemistry of Ni–N compounds is rather rich. In the gas phase, complexes of nickel(II) have been investigated in detail with a variety of nitrogen ligands, such as amines [3–6], amides [7,8], pyridines [9,10], and related *N*-heterocycles [11–14], among which the latter may serve as models for the coordination of nickel with more complex biomolecules. Among these nitrogen containing organic molecules, guanidines represent a very interesting class of compounds due to their high basicity [15] and also their ability to act as monodentate σ-donors in various coordination complexes with metal cations [16–20].

We have recently started [21] an investigation of the gas-phase basicities of several alkyl-substituted guanidines (compounds **1**–**4**, Chart 1) in which the heteroatom-containing sidechains enhance the proton affinities of the compounds compared to other guanidines due to the formation of intramolecular hydrogen bonds (IMHB) [22–24]. The multiple functionalities of guanidines also promote the formation of coordination complexes, and the presence of additional donor ligands in the sidechains is expected to further support this trend. Thus, novel guanidine derivatives bearing an *N*,*N*-dimethylaminopropyl substituent have been used as ligands in copper-based dioxygen activation reactions thus mimicking active site of some enzymes [25]. Furthermore, novel guanidine derivatives bearing *N*,*N*-dialkylaminomethylpyrrolidine substituents were employed in design of chiral zinc/guanidine complexes and tested as enantioselective catalysts in the Henry reaction [26]. In both examples, the guanidine subunit acts as monodentate ligand while the sidechain nitrogen atom provides a second coordination site. A third important aspect is the pronounced tendency of guanidinium ions, i.e. the protonated forms $\mathbf{1}H^+$–$\mathbf{4}H^+$, to form aggregates with oxo-anions via multiple hydrogen bonding [27–29]. Similarly, the formation of anion aggregates may be expected for the metal-cationized forms. Accordingly, protonation and metallation of the free guanidines followed by aggregation of the resulting cationic species with counterions are expected to compete with each other. Here, we report on the coordination chemistry of nickel(II) nitrate with compounds **1**–**4** probed by means of electrospray ionization mass spectrometry (ESI-MS [30–32]), a method for which correlations between the mass spectra and the situation that prevails in solution have been demonstrated to exist [33–37].

* Corresponding authors. Tel.: +385 1 4561 008; fax: +385 1 4680 195.
E-mail addresses: glasovac@emma.irb.hr (Z. Glasovac), schroeder@uochb.cas.cz (D. Schröder).

1387-3806/$ – see front matter © 2009 Elsevier B.V. All rights reserved.
doi:10.1016/j.ijms.2009.11.006

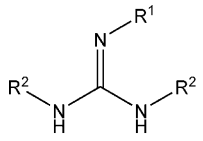

1: $R^1 = (CH_2)_3OCH_3$; $R^2 = (CH_2)_2CH_3$
2: $R^1 = (CH_2)_3N(CH_3)_2$; $R^2 = (CH_2)_2CH_3$
3: $R^1 = (CH_2)_2CH_3$; $R^2 = (CH_2)_3N(CH_3)_2$
4: $R^1 = R^2 = (CH_2)_3N(CH_3)_2$

Chart 1. Structures of the guanidines **1–4**.

2. Experimental and theoretical details

The investigated guanidines **1–4** were prepared according to the previously published procedures and distilled prior to use [38,39]. The ESI-MS experiments were performed with a VG BIO-Q instrument which consists of an ESI source followed by a mass spectrometer of QHQ configuration (Q: quadrupole, H: hexapole) [40]. For each ion of interest, the instrument parameters were optimized for maximum ion abundances by changing from soft to increasingly harsher ionization conditions, as described previously [3,7,41,42]. In the present experiments, mmolar solutions of $Ni(NO_3)_2$ in methanol/water (1:1) were introduced via a syringe pump (flow rate 5 μL/min) to the fused-silica capillary of the ESI source; methanol was used as a co-solvent improving the spray conditions [43]. Nitrogen was used as nebulizing and drying gas at a source temperature of 110 °C. In the ESI mass spectra, the nickel-containing ions are readily identified by their characteristic isotope envelopes [44]. In addition, the possible incorporation of solvent molecules into the ions formed (or isobaric overlaps resulting thereof) were probed by experiments using deuterated methanol as the solvent for ESI [45]. For collision-induced dissociation (CID), the ions of interest were mass-selected using Q1, interacted with xenon in the hexapole collision cell at various collision energies (E_{Lab} = 0–30 eV) at a collision-gas pressure of ca. 3×10^{-4} mbar, while scanning Q2 to monitor the ionic fragments. Note that due to the (approximate) single-collision conditions, a substantial share of the mass-selected parent ions does not undergo any collisions and hence the parent ion intensity decreases to a finite value at high collision energies, rather than vanishing to zero. To a first approximation, the energy dependences of the product distributions can be approximated by a sigmoid function [46], which allows to extract some semi-quantitative information about ion energetics [47]. To this end, the energy dependence of the CID fragments is modeled by functions of the type $I_i(E_{CM}) = (BR_i/(1 + e^{(E_{1/2,i}-E_{CM})b_i}))$ using a least-square criterion; for the parent ion M, the relation is: $I_M(E_{CM}) = [1 - \sum(BR_i/(1 + e^{(E_{1/2,i}-E_{CM})b_i}))]$. Here, BR_i stands for the branching ratio of a particular product ion ($\Sigma BR_i = 1$), $E_{1/2}$ is the energy at which the sigmoid function has reached half of its maximum, E_{CM} is the collision energy in the center-of-mass frame ($E_{CM} = z \times \{m_T/(m_T + m_I)\} \times E_{lab}$, where z is the ion's charge, m_T and m_I stand for the masses of the collision gas and the ion, respectively), and b (in eV^{-1}) describes the rise of the sigmoid curve and thus the phenomenological energy dependence. In consecutive dissociations, all higher-order product ions were added to the intensity of the primary fragment. Further, non-negligible ion decay at E_{lab} = 0 eV as well as some fraction of non-fragmenting parent ions at large collision energies are acknowledged by normalization. Phenomenological appearance energies (AEs) are then derived by linear extrapolation of the rise of the sigmoid curves at $E_{1/2}$ to the base line. This empirical, yet physically reasonable approach is able to reproduce the measured ion yields and thus provides a semi-quantitative framework for the energy demands of the various fragmentations [41,48–51]. In the present study, due to efficient formation of proton-bound dimers, the ion abundances of the nickel-containing complexes of the guanidines **1–4** were rather low. While the uncertainty of the CID data therefore is increased, the main purpose, i.e. a qualitative comparison of **1–4**, is still feasible.

The computational studies were performed with the hybrid density functional method R-B3LYP implemented in the Gaussian 03 program suite [52]. Geometry optimization of all stationary points was performed using Ahlrichs TZVP basis set [53,54], and for each of the complexes described below, several conformations were examined, of which the lowest-energy structures were selected for the discussion. The minima and the transition state (TS) structures on the Born-Oppenheimer potential-energy surfaces were further verified by analysis of the vibrational frequencies. The resulting frequencies were used for the calculation of zero-point energies and thermal corrections without any scaling [55]. The nature of the transition state structures was additionally confirmed by IRC calculations [56,57]. Additionally, geometry optimization of the selected minima was also performed employing broken-symmetry spin unrestricted DFT approach (BS-UDFT) in conjunction with Alrichs TZVP (on Ni, N and O atoms) and SVP (on C and H atoms) basis sets [45] as recommended by Muresan et al. [58]. Molecular structures were viewed and plotted by MOLDEN program [59].

3. Results and discussion

If an aqueous or alcoholic solution of a divalent transition-metal salt MX_2 (X = monovalent counterion) containing a nitrogen ligand L is submitted to ESI-MS, heterolysis of the metal salt and association with the nitrogen ligand usually leads to monocations of the type $[M(L)_mX]^+$ and dications of the type $[M(L)_n]^{2+}$ with $m < n$ [3–14,36,60–62]. With strongly basic amines such as trimethylamine or imidazole, the increased pH value of the solution can sometimes lead to precipitation of metal hydroxides, but by careful dosing of the amine, $[M(L)_mX]^+$ complexes can often still be obtained in reasonable yields [63–67]. In addition to the metal-containing ions, the ESI mass spectra usually show abundant signals for the protonated ligands LH^+ as well as the proton-bound dimers L_2H^+. The formation of these different cationic species in solution can be rationalized by the interplay of heterolytic cleavage of the metal salt (reactions (1) and (2)), followed by association of the solvated ions with the ligand L (reactions (3) and (4)), autoheterolysis of water (reaction (5)), protonation of the ligand (reaction (6)), which consumes protons thereby via the mass-action law produces more free hydroxide ions (reaction (5)) which may in turn lead to the formation of hydroxo complexes (reaction (7)) [34]. Provided that L is a sufficiently strong base, the increase of pH of the solution may finally lead to the precipitation of metal hydroxides (reaction (8)).

$$MX_2 \rightarrow MX^+ + X^- \quad (1)$$

$$MX^+ \rightarrow M^{2+} + X^- \quad (2)$$

$$MX^+ + m\,L \rightarrow [M(L)_mX]^+ \quad (3)$$

$$M^{2+} + n\,L \rightarrow [M(L)_n]^{2+} \quad (4)$$

$$H_2O \rightarrow H^+ + OH^- \quad (5)$$

$$L + H^+ \rightarrow LH^+ \quad (6)$$

$$[M(L)_n]^{2+} + OH^- \rightarrow [M(L)_nOH]^+ \quad (7)$$

$$M^{2+} + 2OH^- \rightarrow M(OH)_2\downarrow \quad (8)$$

Accordingly, ESI of a pure solution of nickel(II) nitrate in methanol/water (1:1) yields abundant monocations of the type $[Ni(NO_3)(CH_3OH)_n]^+$ ($m/z = 120 + 32n$ for the most abundant ^{58}Ni isotope; n = 1–4) as well as metal clusters such as the dinuclear ions $[Ni_2(NO_3)_3(CH_3OH)_n]^+$ ($m/z = 302 + 32n$; n = 2–6) and the trinuclear species $[Ni_3(NO_3)_5(CH_3OH)_n]^+$ ($m/z = 484 + 32n$; n = 3–6) [7,42,62,68]. Further, ESI of the guanidines themselves gives rise to very abundant signals for the protonated compounds LH^+ and

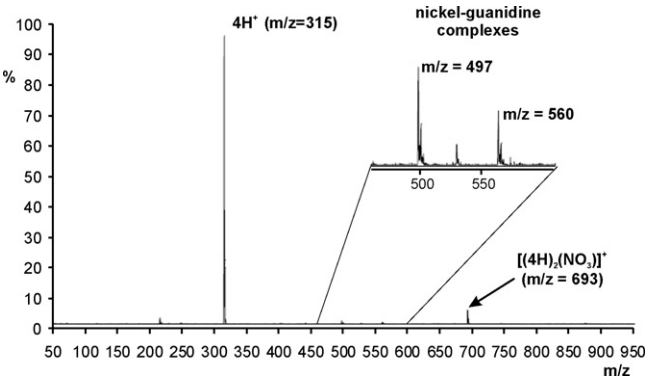

Fig. 1. Representative mass spectrum obtained upon ESI of a dilute methanolic solution of nickel(II) nitrate and the guanidine **4**.

the proton-bound dimers L_2H^+ under soft conditions of ionization [21]. In the presence of nitrate as a counterion of the metal salt, the ion pairs $[(LH)_2(NO_3)]^+$ (Fig. 1) and $[(LH)_3(NO_3)_2]^+$ are also observed under soft ionization conditions which can be ascribed to the general tendency for ion pairing [69] in combination with the specific recognition of oxo-anions by guanidinium ions [27–29]. Although some of these ions arise from the pure components that appear in the same mass regions as the nickel–guanidinium complexes discussed further below, these species can readily be distinguished from each other by their characteristic isotope patterns [44]. Namely, mononuclear nickel complex ions show two signals separated by 2 *m*/*z* units in relative ratio of ca. 3:1, which completely follow theoretical ratio of the most abundant Ni isotopes ^{58}Ni and ^{60}Ni (Fig. 1).

In marked contrast to previous experiments with other nitrogen bases [3–14], ESI of mixtures of the guanidines with nickel(II) nitrate does not afford significant signals of the corresponding $[Ni(L)_mNO_3]^+$ complexes. Instead, at a ca. 1:1 mixing ratio of the metal salt and the guanidine, the spectra show abundant signals due to the individual components (see above), whereas the only ions which contain both, nickel and the guanidines arise from an association of the protonated bases, i.e. guanidinium ions with neutral nickel(II) nitrate. Although we did not optimize the reactant ratio, we noted that the relative increase in nickel nitrate (ca. twofold) did not significantly improve the yield of complex. Before discussing these complexes in more detail further below, let us briefly comment on the absence of the expected $[Ni(L)_mNO_3]^+$ species by reference to reactions (1)–(8). Apparently, at the pH value of the nickel(II) nitrate solution the basicity of the guanidines is so dominant that reaction (6) is completely shifted to the right side and thus no free base is available anymore, and even the presence of nickel(II) ions cannot shift the equilibrium towards coordination according to reactions (3) and (4), respectively. Some other metal salts ($CuSO_4 \times 5H_2O$, $CuCl_2$, $MnCl_2 \times 4H_2O$ and $CoCl_2 \times 6H_2O$) were also tried, but could not be measured via ESI due to precipitation of the hydoxides (reaction (8)) under given conditions.

In the following, we discuss the results obtained for the nickel-containing complexes of the title compounds formed upon electrospray ionization of highly diluted 1:1 mixtures of $Ni(NO_3)_2$ and the guanidines in methanol. We clarify at the outset, however, that the abundances of the resulting complexes containing both nickel and the guanidine samples were moderate to low such that the CID patterns should primarily be compared qualitatively.

In the case of the methoxy compound **1**, an ion with *m*/*z* 676 (for ^{58}Ni) is observed under soft ionization conditions to which – based on ion masses and isotope patterns – we assign the formula $[(\mathbf{1}H)_2Ni(NO_3)_3]^+$. Collision-induced dissociation of the mass-selected ion affords the guanidinium ion $\mathbf{1}H^+$ as the exclusive fragment (Fig. 2a). CID experiments at variable collision energies lead to an apparent threshold for dissociation of only $AE(\mathbf{1}H^+) = (0.1 \pm 0.1)$ eV, and a significant amount of dissociation is already observed at a nominal collision energy of $E_{CM} = 0$ eV. These observations suggest that the species $[(\mathbf{1}H)_2Ni(NO_3)_3]^+$ corresponds to a weakly bound ion pair, which upon CID disintegrates into the components according to reaction (9). A search for ions with a 1:1 ratio of guanidine and nickel (e.g. $[(\mathbf{1}H)Ni(NO_3)_2]^+$, *m*/*z* 398) was not successful, which is consistent with the exclusive occurrence of reaction (9) for the larger ion pair $[(\mathbf{1}H)_2Ni(NO_3)_3]^+$. With regard to the neutral products, we note that the present CID experiments cannot deduce their actual structure. In reaction (9), for example, instead of the three separate fragments $\mathbf{1} + HNO_3 + Ni(NO_3)_2$, the neutral products may also correspond to the ion pair $[(\mathbf{1}H)^+ \cdot NO_3^-]$ concomitant with $Ni(NO_3)_2$ or even the neutral nickel complex $[(\mathbf{1}H)^+ \cdot Ni(NO_3)_3^-]$. Similarly, the product couple $HNO_3 + Ni(NO_3)_2$ may also correspond to $H[Ni(NO_3)_3]$. We note, however, that the binding energies are relatively small and the formation of multiple neutral fragments is preferred entropically (see also Scheme 3 further below). A decision between these options cannot be made currently, however, and therefore in the equations we conservatively list the separate entities in order to avoid any speculation about the existence of the corresponding neutral ion pairs without specific experimental evidence.

$$[(\mathbf{1}H)_2Ni(NO_3)_3]^+ \rightarrow \mathbf{1}H^+ + \mathbf{1} + HNO_3 + Ni(NO_3)_2 \quad (9)$$

$$[(\mathbf{2}H_2)Ni(NO_3)_3]^+ \rightarrow \mathbf{2}H^+ + HNO_3 + Ni(NO_3)_2 \quad (10)$$

For the *N*,*N*-dimethylaminopropyl substituted compound **2**, the most abundant ion containing both nickel and the guanidine corresponds to a formal ion pair with the net composition $[(\mathbf{2}H_2)Ni(NO_3)_3]^+$, *m*/*z* 474. CID of this ion (Fig. 2b) again leads to disintegration with the guanidinium ions as the by far most dominant fragment (reaction (10), $AE = 0.6 \pm 0.2$ eV); at medium collision energies, a trace of $Ni(NO_3)_2$ loss is observed as well. Similar to the results for compound **1**, the energy dependence of the fragmentation yields indicates the presence of a weakly interacting ion pair. At first sight, the ion pairs formed from **1** and **2**, respectively, seem to differ fundamentally (2:1 stoichiometry for the former, 1:1 for the latter), but this difference can be ascribed to the presence of the *N*,*N*-dimethylamino group as an additional strongly basic center in **2**, such that protonation of the remote substituent in **2** fulfills the same function as the second guanidinium cation in $[(\mathbf{1}H)_2Ni(NO_3)_3]^+$.

In contrast to the two former heteroatom-substituted guanidines, the ESI spectra of the *bis*-(*N*,*N*-dimethylaminopropyl) derivative **3** show an ion at *m*/*z* 454 corresponding to $[(\mathbf{3}H)Ni(NO_3)_2]^+$. CID of mass-selected $[(\mathbf{3}H)Ni(NO_3)_2]^+$ (Fig. 2c) leads to sequential expulsions of nitric acid (reactions (11a) and (11b)) as well as a loss of the neutral metal salt (reaction (11c)). Compared to the complexes of compounds **1** and **2**, the fragmentation of $[(\mathbf{3}H)Ni(NO_3)_2]^+$ bears a significantly larger threshold ($AE = 2.2 \pm 0.3$ eV).

$$[(\mathbf{3}H)Ni(NO_3)_2]^+ \rightarrow [(\mathbf{3})Ni(NO_3)]^+ + HNO_3 \quad (11a)$$

$$[(\mathbf{3})Ni(NO_3)]^+ \rightarrow [(\mathbf{3}\text{-}H)Ni]^+ + HNO_3 \quad (11b)$$

$$[(\mathbf{3}H)Ni(NO_3)_2]^+ \rightarrow \mathbf{3}H^+ + Ni(NO_3)_2 \quad (11c)$$

The mere formula of the product ion $[(\mathbf{3})Ni(NO_3)]^+$ formed in reaction (11a) suggest the formation of a genuine coordination complex of the $Ni(NO_3)^+$ fragment with the neutral base and reaction (11b) most probably leads to a guanidate complex. At least upon CID, the *bis*-(*N*,*N*-dimethylaminopropyl) substituted compound accordingly yields coordination complexes rather than ion pairs of the guanidium ions. Interestingly, the branching between reactions (11a) and (11b) implies that the loss of the second HNO_3 molecule is rather facile, because the $[(\mathbf{3}\text{-}H)Ni]^+$ fragment is more abundant than $[(\mathbf{3})Ni(NO_3)]^+$ even at low collision energies.

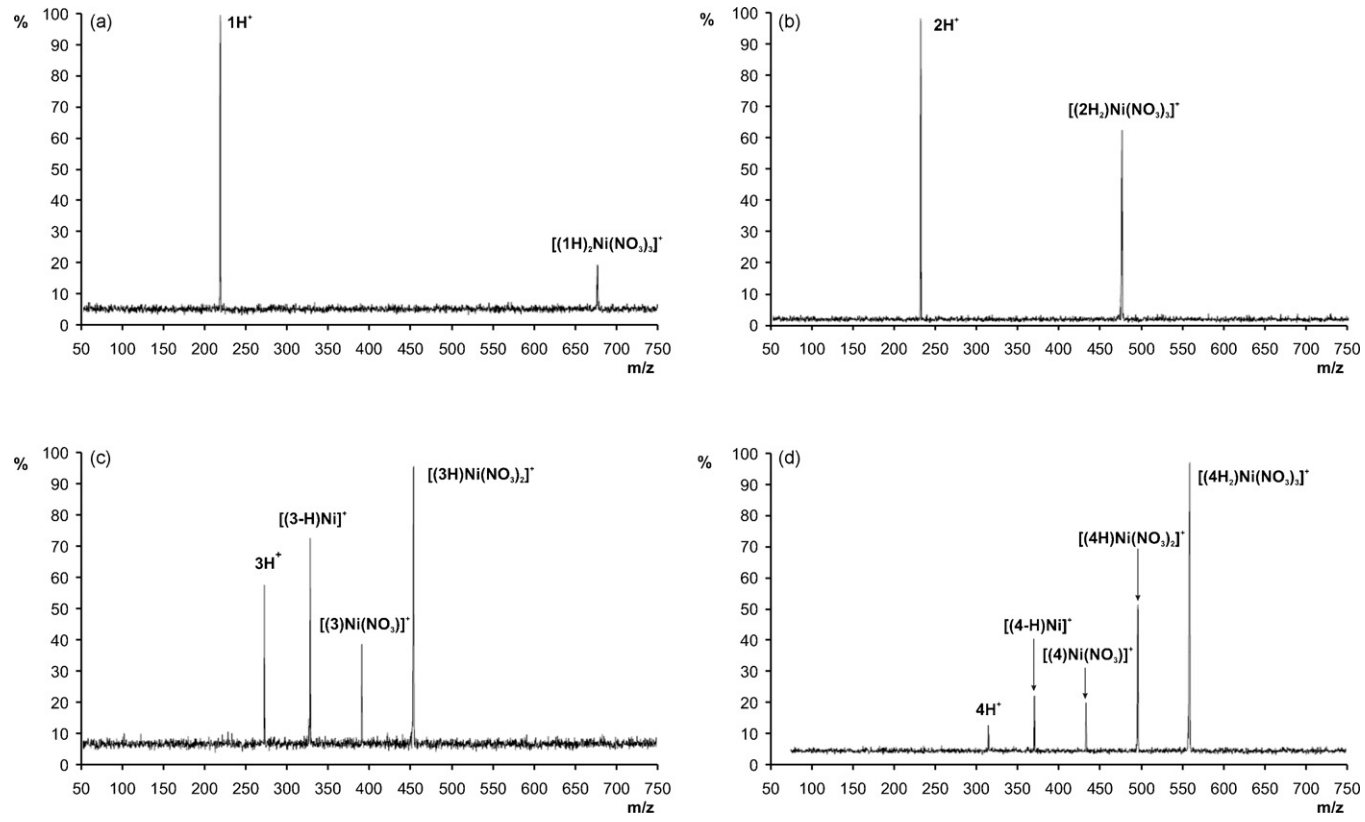

Fig. 2. Representative CID spectra of several nickel/guanidinium complexes recorded at E_{Lab} = 20 eV: (a) mass-selected $[(\mathbf{1}H)_2Ni(NO_3)_3]^+$, (b) mass-selected $[(\mathbf{2}H_2)Ni(NO_3)_3]^+$, (c) mass-selected $[(\mathbf{3}H)Ni(NO_3)_2]^+$ and (d) mass-selected $[(\mathbf{4}H_2)Ni(NO_3)_3]^+$.

Similar to compound **3**, ESI of the *tris*-(*N*,*N*-dimethylaminopropyl) substituted guanidine **4** provides access to coordination complexes of nickel(II), such as $[(\mathbf{4}\text{-H})Ni]^+$ (*m*/*z* 371), $[(\mathbf{4})Ni(NO_3)]^+$ (*m*/*z* 434), $[(\mathbf{4}H)Ni(NO_3)_2]^+$ (*m*/*z* 497), and $[(\mathbf{4}H_2)Ni(NO_3)_3]^+$ (*m*/*z* 560), whose structures can be understood by the occurrence of sequential losses of HNO_3 from the latter species (reactions (12a)–(12c)).

$$[(\mathbf{4}H_2)Ni(NO_3)_3]^+ \rightarrow [(\mathbf{4}H)Ni(NO_3)_2]^+ + HNO_3 \quad (12a)$$

$$[(\mathbf{4}H)Ni(NO_3)_2]^+ \rightarrow [(\mathbf{4})Ni(NO_3)]^+ + HNO_3 \quad (12b)$$

$$[(\mathbf{4})Ni(NO_3)]^+ \rightarrow [(\mathbf{4}\text{-H})Ni]^+ + HNO_3 \quad (12c)$$

$$[(\mathbf{4}H)Ni(NO_3)_2]^+ \rightarrow \mathbf{4}H^+ + Ni(NO_3)_2 \quad (12d)$$

This interpretation of the ion-source mass spectra is consistent with the results obtained upon CID of mass-selected $[(\mathbf{4}H_2)Ni(NO_3)_3]^+$ (Fig. 2d). Thus, loss of the first HNO_3 molecule (reaction (12a)) is rather facile (*AE* = 0.3 ± 0.2 eV), whereas the subsequent expulsions of nitric acid (reactions (12b) and (12c)) as well as formation of the guanidinium ion (reaction (12d)) have thresholds lying above 1 eV. As a representative example, Fig. 3 shows the energy dependence of the fragmentation of the parent ion $[(\mathbf{4}H_2)Ni(NO_3)_3]^+$ at variable collision energies. Although the loss of the first HNO_3 molecule is facile under low-energy CID experiments, the parent ion does not completely disappear at high collision energies, which is a direct consequence of the fact that the CID experiments were performed at (approximate) single-collision conditions, which implies that a significant fraction of the parent ions does not experience any collision at all and hence also does not fragment.

In comparison, the four substituted guanidines investigated in this work show significant differences in their coordination ability towards Ni(II) ions. Specifically, due to their large basicities, the guanidines have a large tendency for protonation under the conditions applied and thus cannot coordinate to the metal cation by the lone pair of the imino nitrogen. Instead, ion-pair complexes of the guanidinium ions with neutral nickel(II) nitrate are formed via the nitrate counterions as a linkage. Without additional substituents, these ion pairs disintegrate upon CID to afford the guanidinium ions as the exclusive charged fragments. Only if sufficiently strong donor ligands are present in the side chain, i.e. in the case of compounds **3** and **4**, genuine coordination complexes of Ni(II) are formed. Apparently, neither the presence of only one

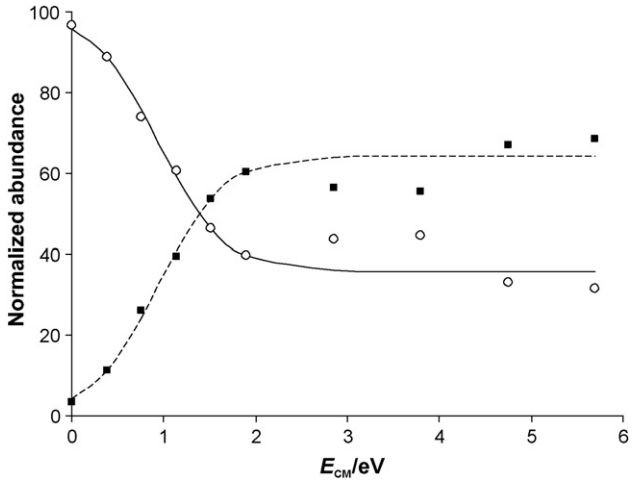

Fig. 3. Energy-dependent CID breakdown diagram of mass-selected $[(\mathbf{4}H_2)Ni(NO_3)_3]^+$ as a function of the collision energy given in the center-of-mass frame; here, the parent ion (○) and the sum of fragment ions (■) are shown normalized to Σ = 100.

Table 1a
Electronic (E_{el} and E_{tot}) and total Gibbs energies (G_{tot}) and relative stabilities (ΔE_{rel} and ΔG_{rel}) of the investigated structures calculated using the R-B3LYP/TZVP approach.

Molecules	E_{el}/a.u.	E_{ZPV}/a.u. (G_{corr}/a.u.)[c]	E_{0K°/a.u. (G_{298K°/a.u.)	ΔE_{rel}[a] (ΔG_{rel})	$\Delta_r G$[a,b]
$Ni(NO_3)_2$	−2069.23586	0.03345 (−0.00051)	−2069.20241 (−2069.23636)		
HNO_3	−280.99523	0.02611 (0.00034)	−280.96912 (−280.99489)		
4H$^+$	−961.84182	0.56919 (0.51552)	−961.27263 (−961.32630)		
C4a	−3312.11711	0.63512 (0.55246)	−3311.48199 (−3311.56465)	0.0 (0.0)	4.6
C4b	−3312.11672	0.63289 (0.55849)	−3311.48384 (−3311.55823)	−1.2 (4.0)	0.5
C4c	−3312.10387	0.63751 (0.56421)	−3311.46636 (−3311.53966)	9.8 (15.7)	−11.1
F1	−3031.09113	0.60276 (0.52864)	−3030.48837 (−3030.56249)		0.4
F2	−2750.07671	0.57450 (0.50967)	−2749.50221 (−2749.56704)		15.4
F3	−2469.03942	0.54724 (0.49189)	−2468.49219 (−2468.54754)		

[a] Relative electronic and Gibbs energies as well as the Gibbs reaction energies (ΔE_{rel}, ΔG_{rel} and $\Delta_r G$) are given in kcal mol^{-1}.
[b] Gibbs reaction energies for loss of one molecule of nitric acid from the respective complex.
[c] G_{corr} represent Gibbs correction of the electronic energy to 298 K and is calculated by equation: $G_{corr} = E_{ZPV} + RT - TS$.

additional *N*,*N*-dimethylaminopropyl substituent in compound **2** nor the methoxypropyl substitution in **1** lead to sufficiently stable complexes.

In order to gain further insight, compound **4** was selected for an exploratory computational study using density functional theory. The possible structures of the experimentally observed complex [(**4**H$_2$)Ni(NO$_3$)$_3$]$^+$ comprising the guanidine **4** and nickel nitrate were calculated using the R-B3LYP/TZVP and BS-UDFT approaches (Tables 1a and 1b, respectively). Starting with a number of possible geometries of the observed ion [(**4**H$_2$)Ni(NO$_3$)$_3$]$^+$, we identified three groups of structures with respect to bonding pattern of nitrate anions. In the further discussion, only the lowest-energy minima in each group (**C4a**–**C4c**, Fig. 4) are considered.

For [(**4**H$_2$)Ni(NO$_3$)$_3$]$^+$, the calculations predict ion-pair complexes as the most stable structures in which at least one nitrate ion acts as a bridging counterion for the guanidinium center and the remotely protonated *N*,*N*-dimethylamino group via two hydrogen bonds. The nickel(II) is coordinated to the remaining *N*,*N*-dimethylamino donor ligands and the nitrato ligands (Fig. 4). Although the geometrical arrangement of **C4a** closely resembles structures of previously published similar complexes [25,26], we disregard it for two reasons. Firstly, in **C4a**, the N1-atom of the guanidine subunit is not protonated and instead includes an interaction of a Ni(NO$_3$)$^+$ cation with neutral guanidine as a primary process. Additionally, two outer amino nitrogen atoms are protonated which can occur only if the protonation is a consequence of binding of two molecules of nitric acid after the Ni-guanidine bond is established. This reaction scheme is highly unlikely in view of other experimental data which indicate that protonation of guanidine subunit strongly dominates over all other possible reaction channels. The second argument against structure **C4a** comes from the CID experiments. Upon low-energy fragmentation of **C4a**, one can expect two nearly equivalent losses of HNO_3 molecules, in contrast to the experimental finding. Instead, structures **C4b** and **C4c** are fully consistent with observed low-energy fragmentation pattern. More precisely, in these two structures only one nitrate is incorporated in an intramolecular hydrogen bond and we propose that this nitrate unit is involved in the first elimination of HNO_3.

Table 1b
BS-UDFT results.

Molecules	E_{el}/a.u.	E_{ZPV}/a.u. (G_{corr}/a.u.)[c]	E_{0K°/a.u. (G_{298K°/a.u.)	ΔE_{rel}[a] (ΔG_{rel})	$\Delta_r G$[a,b]
$Ni(NO_3)_2$	−2069.23586	0.03345 (−0.00051)	−2069.20241 (−2069.23636)		
HNO_3	−280.99244	0.02599 (0.00023)	−280.96645 (−280.99221)		
4H$^+$	−961.15561	0.56635 (0.51233)	−960.58926 (−960.64328)		
C4a	−3311.42653	0.62955 (0.54869)	−3310.79698 (−3310.87784)	0.0 (0.0)	−2.4
C4b	−3311.42905	0.62930 (0.54814)	−3310.79975 (−3310.88091)	−1.7 (−1.9)	−0.5
C4c	−3311.41758	0.63347 (0.55938)	−3310.78410 (−3310.85820)	8.1 (12.3)	11.9
F1	−3030.40661	0.60180 (0.53001)	−3029.80481 (−3029.87660)		7.6
F2	−2749.39329	0.57190 (0.50695)	−2748.82139 (−2748.88634)		−1.2
F3	−2468.35733	0.54534 (0.49032)	−2467.81199 (−2467.86700)		17.0

[a] Relative electronic and Gibbs energies as well as the Gibbs reaction energies (ΔE_{rel}, ΔG_{rel} and $\Delta_r G$) are given in kcal mol^{-1}.
[b] Gibbs reaction energies for loss of one molecule of nitric acid from the respective complex.
[c] G_{corr} represent Gibbs correction of the electronic energy to 298 K and is calculated by equation: $G_{corr} = E_{ZPV} + RT - TS$.

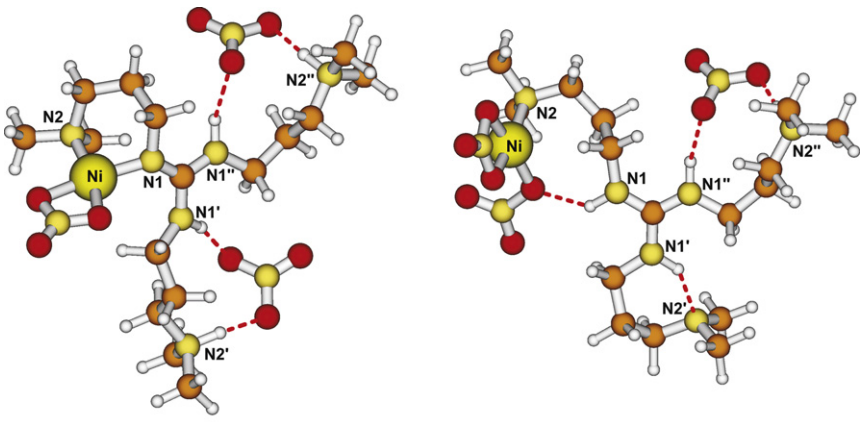

$\Delta_r G$	C4a	C4b	C4c
R-B3LYP	0.0	4.0	15.7
BS-UB3LYP	(0.0)	(-1.9)	(12.3)

Fig. 4. Relative Gibbs energies (in kcal mol^{-1}) of the three lowest-energy structures of the complex [(**4**H$_2$)Ni(NO$_3$)$_3$]$^+$ optimized at the R-B3LYP/TZVP level of theory; values in parentheses refer to BS-UDFT results.

To check this assumption, we calculated the activation energies (E_a) for the two fragmentation channels represented by reaction pathways *A* and *B* using somewhat smaller model systems (Scheme 1); they serve to describe losses of chemically different molecules of nitric acid from the complexes **M1–M3** as simplified analogues of **C4b** and **C4c** (Table 2). For the reaction pathways *A* and *B*, fragmentation can be divided in two processes: (i) isomerization of the starting complex to the proton-bound dimer and (ii) fragmentation of the proton-bound dimer formed. The process (ii) is generally considered as the process with low or no barrier. For this reason we assumed isomerization as the rate determining step for the fragmentation of nitrates from the investigated complexes. Structures **M1** and **M2** were derived from structure **C4b** assuming a mutual independence of the fragmentation pathways of the two significantly different nitrates: one shared between nickel and guanidine and the second involved in two hydrogen bonds. These calculations predict the fragmentation channel *B* to be energetically favorable by 23 kcal mol^{-1} what corroborates our above deduction. In addition, another minimum is identified (**M1**$_{IM}$) on path *A* indicating that elimination of nitric acid is not a single-step process; the second barrier is calculated to be lower than the first one by 8 kcal mol^{-1}.

Further, we recall from the experimental data that the presence of at least two dimethylaminopropyl chains is required for the formation of stable nickel complexes, corroborating **C4b** and **C4c** as the most conceivable structures. Elimination of nitric acid from **C4c** was also tried, but the efforts to locate transition structures for this process resulted in a scission of the (CH$_3$)$_2$N–Ni bond (marked with "*a*", see fragmentation pathway *C* in Scheme 1) thus leading to a rearranged structure analogous to **C4b**. For this purpose two isomers (**M3** and **M3′**, see Scheme 2) were considered. The orientations of the nitrate ion in structures **M3** and **M3′** are chosen to follow structural patterns in **C4b** and **C4c**. Since there is no significant energy difference between these two minima (ca. 0.1 kcal mol^{-1}), we choose **M3** structure as a starting point for the saddle-point calculations. While attempts to fully optimize **TS3** were unsuccessful, approximate geometry and energy of **TS3** was obtained

Table 2
Activation energies obtained for the fragmentation of investigated complexes calculated at the R-B3LYP/TZVP level of theory.

	E_{el}/a.u.	E_{ZPV}/a.u.	$E_{0\,K}$/a.u.	E_a/kcal mol^{-1}
M1	−2605.74358	0.34064	−2605.40295	
TS1	−2605.68463	0.33777	−2605.34687	35.2[a]
M1$_{IM}$	−2605.70888	0.34070	−2605.36819	
TS1a	−2605.69895	0.33824	−2605.36071	26.5[a]
M1$_P$	−2605.72388	0.34075	−2605.38313	
M2	−817.51254	0.33430	−817.17824	
TS2	−817.48975	0.33082	−817.15893	12.1[b]
M2$_P$	−817.49053	0.33075	−817.15978	
M3	−2818.40383	0.47605	−2817.92779	
M3′	−2818.40228	0.47579	−2817.92650	
TS3	−2818.38568	0.47314	−2817.91254	8.8 (9.6)[c]
M3$_P$	−2818.41038	0.47144	−2817.93894	−7.0[c]

[a] Relative to structure **M1**.
[b] Relative to structure **M2**.
[c] Relative to **M3** and **M3′** structures with the latter being parenthesized.

Fragmentation pathway A:

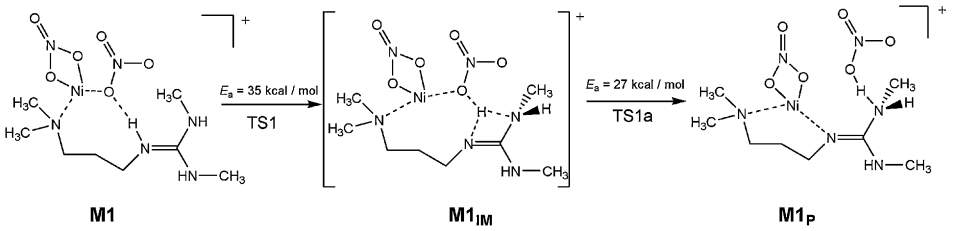

$\Delta_r G$(**M1**→**M1p**) = 10.8 kcal mol^{-1}

Fragmentation pathway B:

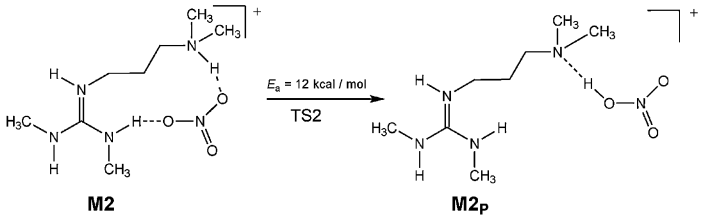

$\Delta_r G$(**M2**→**M2p**) = 8.3 kcal mol^{-1}

Fragmentation pathway C: (scission of Ni-N bond "a")

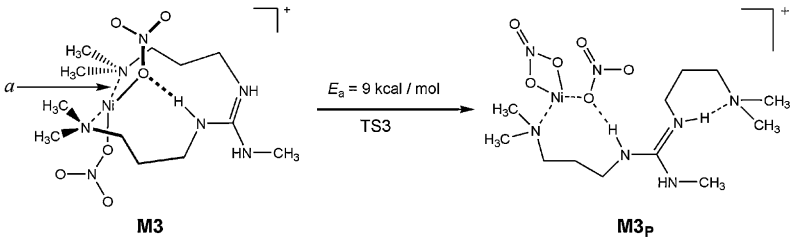

$\Delta_r G$(**M3**→**M3p**) = -12.1 kcal mol^{-1}

Scheme 1. Calculated activation energies (E_a) for the competing isomerization pathways preceding the extrusion of nitric acid from model complex structures **M1** and **M2** derived from **C4b** (paths *A* and *B*). In the case of pathway *C*, E_a was estimated from relaxed scan calculation of the reaction coordinate. The energy difference between two isomers described by different N–H···O hydrogen bonding is less than 1 kcal mol^{-1}.

by a series of constrained optimization steps until the energy gradient along the frozen internal coordinate (N–Ni bond) was less than 10^{-3} a.u/Bohr. The nature of this stationary point was verified by a vibrational analysis (N_{imag} = 1) and IRC calculations [56,57] which led to the reactant **M3** and the product **M3p**, as expected. Such constrained optimization resulted in an estimated activation energy of 8.8 kcal mol^{-1} for this particular process, which is even lower than $E_a(B)$. These findings suggest that structure **C4c** is most likely formed at the initial stage of ion aggregation, but it can easily rearrange to the more stable isomer **C4b** under the experimental conditions.

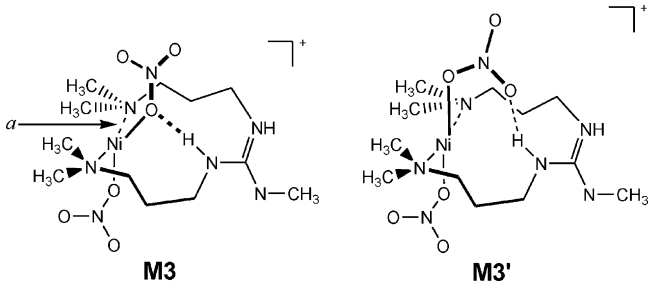

Scheme 2. Representation of two possible minima considered as the model structures for calculation of the fragmentation pathway *C*.

Inspired by these findings, in the following we consider **C4b** as the most probable structure of our target complex. The Gibbs energy of formation for the complex **C4b** amounts −2.4 kcal mol^{-1}, and reaction (13) in Scheme 3 is thus almost thermoneutral; this may explain the low abundance of the corresponding complexes formed upon electrospray ionization. Extrusion of the first molecule of nitric acid from the ion **C4b** affords the ion $[(\mathbf{4}H)Ni(NO_3)_2]^+$, whose geometry optimization leads to structure **F1** (Fig. 5) as the most stable minimum. Subsequent elimination of nitric acid starting from **F1** is accompanied by deprotonation of the guanidine moiety and establishing an Ni–N_{imino} bond in structure **F2**. Finally, deprotonation of the guanidine subunit occurs upon extrusion of the third nitrato ligand. The guanidate ion formed acts as a bidentate ligand, while other two coordination places are occupied by two sidechain amino nitrogen atoms (structure **F3**).

This analysis can explain most of the experimental results, but the inspection of the reaction Gibbs energies given in Scheme 3 does not account for the differential fragmentation thresholds experimentally observed for the first and second loss of HNO_3 from $[(\mathbf{4}H)Ni(NO_3)_2]^+$. Specifically, while the experiments indicate a significantly lower threshold for the loss of the first HNO_3 molecule, the calculations predict the two consecutive extrusions of nitric acid (reactions (14) and (15) in Scheme 3) to occur simultaneously at low energies. However, the calculated reaction barriers for these

$$_4H^+ + HNO_3 + Ni(NO_3)_2 \xrightarrow{{}_rG = -0.4\ (-3.5)} [(_4H_2)Ni(NO_3)_3]^+ \quad (13)$$
C4b

$$[(_4H_2)Ni(NO_3)_3]^+ \xrightarrow{{}_rG = 0.6\ (7.6)} [(_4H)Ni(NO_3)_2]^+ + HNO_3 \quad (14)$$
C4b **F1**

$$[(_4H)Ni(NO_3)_2]^+ \xrightarrow{{}_rG = 0.4\ (-1.2)} [(_4)Ni(NO_3)]^+ + HNO_3 \quad (15)$$
F1 **F2**

$$[(_4H)Ni(NO_3)_2]^+ \xrightarrow{{}_rG = -0.1\ (-4.1)} {}_4H^+ + Ni(NO_3)_2 \quad (16)$$
F1

$$[(_4)Ni(NO_3)]^+ \xrightarrow{{}_rG = 15.4\ (17.0)} [(_4\text{-}\mathbf{H})Ni]^+ + HNO_3 \quad (17)$$
F2 **F3**

Scheme 3. Calculated reaction Gibbs energies (in kcal mol^{-1}) for the formation and fragmentation of nickel–guanidine complex **C4b** as calculated at the R-B3LYP/TZVP level of theory; BS-UDFT results are given in parentheses.

two fragmentation steps (Scheme 1) are markedly different, what is consistent with a significantly higher threshold for the loss of the second molecule of nitric acid.

Finally, we should briefly comment possibility of reduction of Ni(II) to Ni(I) upon CID experiments. It has been shown earlier that in electrospray spectra of Ni(II) salts with amino acids, nickel atom remains in the (II+) oxidation state [70]. Similarity of the NPA and Mulliken net charges at nickel along the series of complexes indicate no changes in the formal oxidation states of the metal. More precisely, NPA charges vary from 1.03 (**C4a**) to 0.92 (**F3**) what is

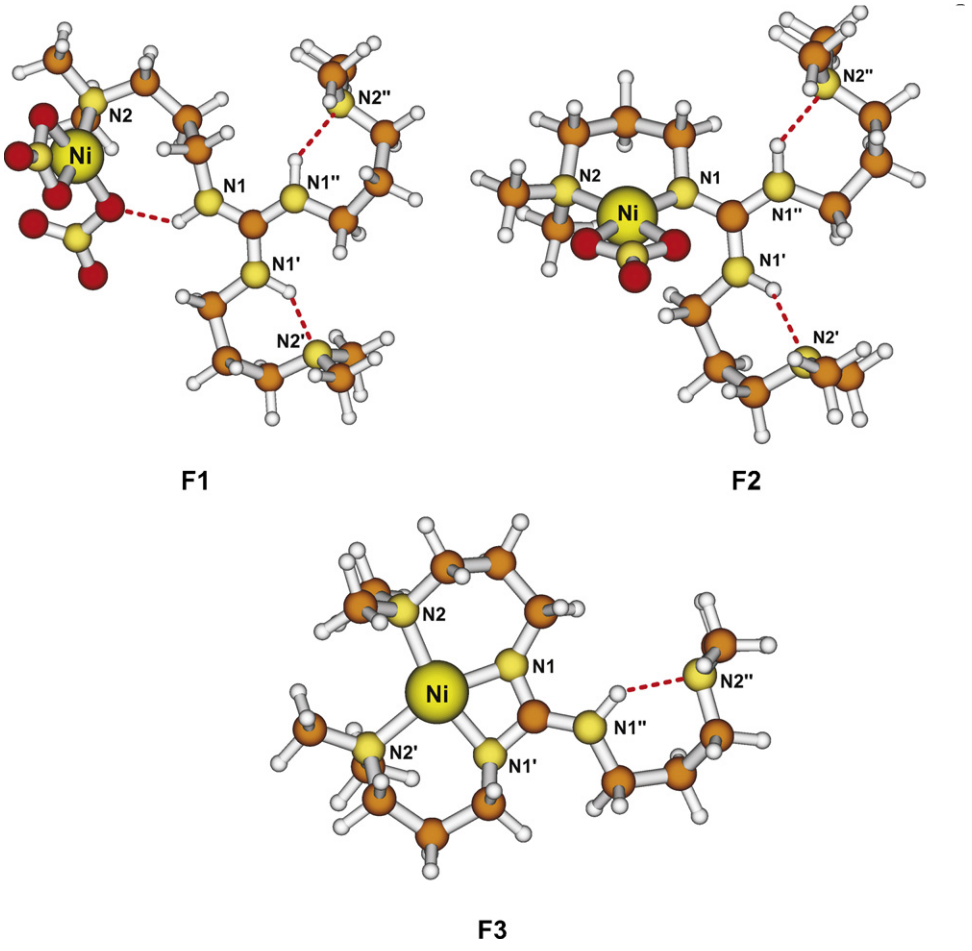

Fig. 5. R-B3LYP structures of the fragments **F1–F3** evolving upon consecutive losses of neutral HNO_3 molecules from the $[(\mathbf{4}H_2)Ni(NO_3)_3]^+$ complex **C4b**.

similar to the net charge in nickel nitrate (1.02). In this context we should note that upon explicit testing of the wavefunction of the ion **F3**, no instability issues were found and the wavefunction possess the properties of the fully spin-paired one. A more detailed elucidation of this aspect could be achieved by means of MS3 experiments which are beyond the scope of the paper because of the low abundances of the ions of interest upon ESI as well as the fact that a other instrumentation would have been required (e.g. an ion trap [71–73]) because the QHQ mass spectrometer used here maximally allows MS/MS studies.

4. Conclusions

The coordination chemistry of nickel(II) with selected heteroatom substituted guanidines is investigated by means of electrospray ionization mass spectrometry. Due to the large basicities of the guanidines, the tendency for protonation of the bases to the corresponding guanidinium ions is rather high and effectively prevents formation of genuine coordination complexes of the type $Ni(L)_n^{2+}$. Instead, ion-pair complexes are formed which formally comprise two organic cations and a $Ni(NO_3)_3^-$ counterion. Collisional activation of these ion-pair complexes leads to the bare guanidinium ions, unless the sidechains of the bases bear additional donor substituents which can promote coordination of nickel(II). These observations suggest that the investigated guanidines with two or three *N*,*N*-dimethylamino groups can act as bidentate or even as tridentate ligands, which results in formation of sufficiently stable Ni(II) complexes. Besides, the *tris*-(3-dimethylaminopropyl) derivative **4** acts as a ligand in which one part of the molecule interacts with anion while the other part ligates to metal cation. Guanidines with a single *N*,*N*-dimethylaminopropyl substitent or a methoxypropyl group within the sidechain do not form similar coordination complexes with nickel(II) and instead loose the neutral metal salt concomitant with formation of the protonated base.

Acknowledgments

This work was supported by the DAAD project “Experimental and computational study of protonated organic molecules”. Additional support was provided by the Czech Academy of Sciences (Z40550506), the Deutsche Forschungsgemeinschaft, the European Reasearch Council (AdG HORIZOMS), the, Grant Agency of the Czech Republic (203/08/1487), and the Ministry of Science, Education, and Sport of Croatia (098-0982933-2920). We would also like to thank the Computing Center of the University of Zagreb (SRCE) for allocation of computer time on the Isabella cluster.

References

[1] M. Schlangen, Ph.D. Thesis, TU Berlin D83, 2008.
[2] O. Mó, M. Yañez, J.Y. Salpin, J. Tortajada, Mass Spectrom. Rev. 26 (2007) 474.
[3] N.G. Tsierkezos, D. Schröder, H. Schwarz, Int. J. Mass Spectrom. 235 (2004) 33.
[4] T. Mitkina, V. Fedin, R. Llusar, I. Sorribes, C. Vicent, J. Am. Soc. Mass Spectrom. 18 (2007) 1863.
[5] J. Anichina, D.K. Bohme, Int. J. Mass Spectrom. 267 (2007) 256.
[6] A.M. Lamsabhi, O. Mo, M. Yañez, J.Y. Salpin, V. Haldys, J. Tortajada, J.C. Guillemin, J. Phys. Chem. A 112 (2008) 10509.
[7] N.G. Tsierkezos, D. Schröder, H. Schwarz, J. Phys. Chem. A 107 (2003) 9575.
[8] T.J. Shi, K.W.M. Siu, A.C. Hopkinson, Int. J. Mass Spectrom. 255 (2006) 251.
[9] M.T. Rodgers, J.R. Stanley, P.B. Armentrout, J. Am. Chem. Soc. 122 (2000) 10969.
[10] N.S. Rannulu, M.T. Rodgers, J. Phys. Chem. A 113 (2009) 4534.
[11] R. Amunugama, M.T. Rodgers, J. Phys. Chem. A 105 (2001) 9883.
[12] M.J.Y. Jarvis, L.F. Pisterzi, V. Blagojevic, G.K. Koyanagi, D.K. Bohme, Int. J. Mass Spectrom. 227 (2003) 161.
[13] M.J.Y. Jarvis, V. Blagojevic, G.K. Koyanagi, D.K. Bohme, Eur. J. Mass Spectrom. 10 (2004) 949.
[14] N.S. Rannulu, M.T. Rodgers, Phys. Chem. Chem. Phys. 7 (2005) 1014.
[15] T. Ishikawa (Ed.), Superbases for Organic Chemistry, J. Wiley and Sons Ltd., Chichester, 2009, and references cited therein.
[16] P.J. Bailey, S. Pace, Coord. Chem. Rev. 214 (2001) 91.
[17] H. Wittmann, V. Raab, A. Schorm, J. Plackmeyer, J. Sundermeyer, Eur. J. Inorg. Chem. (2001) 1937.
[18] V. Raab, J. Kipke, O. Burghaus, J. Sundermeyer, Inorg. Chem. 40 (2001) 6964.
[19] S.H. Oakley, D.B. Soria, M.P. Coles, P.B. Hitchcock, Polyhedron 25 (2006) 1247.
[20] S. Aoki, K. Iwaida, N. Hanamoto, M. Shiro, E. Kimura, J. Am. Chem. Soc. 124 (2002) 5256.
[21] Z. Glasovac, V. Štrukil, M. Eckert-Maksić, D. Schröder, M. Kacorowska, H. Schwarz, Int. J. Mass Spectrom. 270 (2008) 39.
[22] R.W. Alder, Chem. Rev. 89 (1989) 1215.
[23] B. Kovačević, Z. Glasovac, Z.B. Maksić, J. Phys. Org. Chem. 15 (2002) 765.
[24] Z.B. Maksić, Z. Glasovac, I. Despotović, J. Phys. Org. Chem. 15 (2002) 499.
[25] S. Herres-Pawlis, P. Verma, R. Haase, P. Kang, C.T. Lyons, E.C. Wasinger, U. Flörke, G. Henkel, T.D.P. Stack, J. Am. Chem. Soc. 131 (2009) 1154.
[26] U. Köhn, M. Schulz, H. Görls, E. Anders, Tetrahedron: Asymmetry 16 (2005) 2125.
[27] F.P. Schmidtchen, Coord. Chem. Rev. 250 (2006) 2918.
[28] C. Schmuck, Coord. Chem. Rev. 250 (2006) 3053.
[29] P. Blondeau, M. Segura, R. Perez-Fernandez, J. de Mendoza, Chem. Soc. Rev. 36 (2007) 198.
[30] M. Yamashita, J.B. Fenn, J. Phys. Chem. 88 (1984) 4451.
[31] J.B. Fenn, J. Am. Soc. Mass Spectrom. 4 (1993) 524.
[32] P. Jayaweera, A.T. Blades, M.G. Ikonomou, P. Kebarle, J. Am. Chem. Soc. 112 (1990) 2452.
[33] V.B. Di Marco, G.G. Bombi, Mass Spectrom. Rev. 25 (2006) 347.
[34] T. Urabe, T. Tsugoshi, M. Tanaka, J. Mass. Spectrom. 44 (2009) 193.
[35] R. Franski, G. Schroeder, B. Gierczyk, P. Niedzialkowski, T. Ossowski, Int. J. Mass Spectrom. 266 (2007) 180.
[36] N.G. Tsierkezos, J. Roithová, D. Schröder, I.E. Molinou, H. Schwarz, J. Phys. Chem. B 112 (2008) 4365.
[37] N.G. Tsierkezos, J. Roithová, D. Schröder, M. Ončák, P. Slavíček, Inorg. Chem. 48 (2009) 6287.
[38] M. Eckert-Maksić, Z. Glasovac, P. Trošelj, A. Kütt, T. Rodima, I. Koppel, I.A. Koppel, Eur. J. Org. Chem. (2008) 5176.
[39] Z. Glasovac, B. Kovačević, E. Meštrović, M. Eckert-Maksić, Tetrahedron Lett. 46 (2005) 8733.
[40] D. Schröder, T. Weiske, H. Schwarz, Int. J. Mass Spectrom. 219 (2002) 729.
[41] C. Trage, M. Diefenbach, D. Schröder, H. Schwarz, Chem. Eur. J. 12 (2006) 2454.
[42] J. Roithová, D. Schröder, J. Am. Chem. Soc. 129 (2007) 15311.
[43] N.B. Cech, C.G. Enke, Mass Spectrom. Rev. 20 (2001) 362.
[44] Calculated using the Chemputer made by M. Winter, University of Sheffield, see: http://winter.group.shef.ac.uk/chemputer/.
[45] S. Feyel, D. Schröder, H. Schwarz, J. Phys. Chem. A 110 (2006) 2647.
[46] G. Bouchoux, D. Leblanc, J.Y. Salpin, Int. J. Mass Spectrom. 153 (1996) 37.
[47] D. Schröder, M. Engeser, M. Brönstrup, C. Daniel, J. Spandl, H. Hartl, Int. J. Mass Spectrom. 228 (2003) 743.
[48] P. Gruene, C. Trage, D. Schröder, H. Schwarz, Eur. J. Inorg. Chem. (2006) 4546.
[49] D. Schröder, M. Engeser, H. Schwarz, E.C.E. Rosenthal, J. Döbler, J. Sauer, Inorg. Chem. 45 (2006) 6235.
[50] J. Roithová, D. Schröder, J. Míšek, I.G. Stará, I. Starý, J. Mass Spectrom. 42 (2007) 1233.
[51] B. Jagoda-Cwiklik, P. Jungwirth, L. Rulíšek, P. Milko, J. Roithová, J. Lemaire, P. Maitre, J.M. Ortega, D. Schröder, ChemPhysChem 8 (2007) 1629.
[52] M.J. Frisch, G.W. Trucks, H.B. Schlegel, G.E. Scuseria, M.A. Robb, J.R. Cheeseman, J.A. Montgomery, Jr., T. Vreven, K.N. Kudin, J.C. Burant, J.M. Millam, S.S. Iyengar, J. Tomasi, V. Barone, B. Mennucci, M. Cossi, G. Scalmani, N. Rega, G.A. Petersson, H. Nakatsuji, M. Hada, M. Ehara, K. Toyota, R. Fukuda, J. Hasegawa, M. Ishida, T. Nakajima, Y. Honda, O. Kitao, H. Nakai, M. Klene, X. Li, J.E. Knox, H.P. Hratchian, J.B. Cross, C. Adamo, J. Jaramillo, R. Gomperts, R.E. Stratmann, O. Yazyev, A.J. Austin, R. Cammi, C. Pomelli, J.W. Ochterski, P.Y. Ayala, K. Morokuma, G.A. Voth, P. Salvador, J.J. Dannenberg, V.G. Zakrzewski, S. Dapprich, A.D. Daniels, M.C. Strain, O. Farkas, D.K. Malick, A.D. Rabuck, K. Raghavachari, J.B. Foresman, J.V. Ortiz, Q. Cui, A.G. Baboul, S. Clifford, J. Cioslowski, B.B. Stefanov, G. Liu, A. Liashenko, P. Piskorz, I. Komaromi, R.L. Martin, D.J. Fox, T. Keith, M.A. Al-Laham, C.Y. Peng, A. Nanayakkara, M. Challacombe, P.M.W. Gill, B. Johnson, W. Chen, M.W. Wong, C. Gonzalez, J.A. Pople, Gaussian 03, Revision B.03, Gaussian Inc., Pittsburgh, PA, 2003.
[53] A. Schäfer, C. Huber, R. Ahlrichs, J. Chem. Phys. 100 (1994) 5829.
[54] A. Schäfer, H. Horn, R. Ahlrichs, J. Chem. Phys. 97 (1992) 2571.
[55] A.P. Scott, L. Radom, J. Phys. Chem. 100 (1996) 16502.
[56] C. Gonzales, H.B. Schlegel, J. Chem. Phys. 90 (1989) 2154.
[57] C. Gonzales, H.B. Schlegel, J. Chem. Phys. 94 (1990) 5523.
[58] N. Muresan, K. Chlopek, T. Weyhermüller, F. Neese, F. Wieghardt, Inorg. Chem. 46 (2007) 5327.
[59] G. Schaftenaar, J.H. Noordik, J. Comp. Aided Mol. Design 14 (2000) 123.
[60] A.T. Blades, P. Jayaweera, M.G. Ikonomou, P. Kebarle, Int. J. Mass Spectrom. 102 (1990) 251.
[61] M. Kohler, J.A. Leary, J. Am. Soc. Mass Spectrom. 8 (1997) 1124.
[62] N.G. Tsierkezos, M. Diefenbach, J. Roithová, D. Schröder, H. Schwarz, Inorg. Chem. 44 (2005) 4969.
[63] D. Schröder, H. Schwarz, Int. J. Mass Spectrom. 227 (2003) 121.
[64] D. Schröder, H. Schwarz, S. Schenk, E. Anders, Angew. Chem. Int. Ed. 42 (2003) 5087.
[65] R. Franski, K. Klonowska-Wieszczycka, A. Borowiak-Resterna, A. Szanowski, Eur. J. Mass Spectrom. 12 (2006) 311.

[66] P. Milko, J. Roithová, N.G. Tsierkezos, D. Schröder, J. Am. Chem. Soc. 130 (2008) 7186.
[67] A. Revesz, P. Milko, J. Roithová, D. Schröder, J. Mass Spectrom., submitted for publication.
[68] D. Schröder, K.P. de Jong, J. Roithová, Eur. J. Inorg. Chem. (2009) 2121.
[69] Y. Marcus, G. Hefter, Chem. Rev. 106 (2006) 4585.
[70] T. Yalcin, J. Wang, D. Wen, A.G. Harrison, J. Am. Soc. Mass Spectrom. 8 (1997) 749.
[71] R.A.J. O'Hair, Chem. Commun. (2006) 1469.
[72] A. Tintaru, J. Roithová, D. Schröder, L. Charles, I. Jušinski, Z. Glasovac, M. Eckert-Maksić, J. Phys. Chem. 112 (2008) 12097.
[73] E.C. Tyo, A.W. Castleman Jr., D. Schröder, P. Milko, J. Roithová, J.M. Ortega, M.A. Cinellu, F. Cocco, G. Minghetti, J. Am. Chem. Soc. 131 (2009) 13009.